

PREPARED FOR SUBMISSION TO JCAP

CTPU-15-03
IPMU15-0031

Gravitational waves from domain walls in the next-to-minimal supersymmetric standard model

Kenji Kadota,^a Masahiro Kawasaki,^{b,c} and Ken'ichi Saikawa^d

^aCenter for Theoretical Physics of the Universe,
Institute for Basic Science, Daejeon 305-811, Korea

^bInstitute for Cosmic Ray Research, The University of Tokyo,
5-1-5 Kashiwa-no-ha, Kashiwa City, Chiba 277-8582, Japan

^cKavli Institute for the Physics and Mathematics of the Universe (WPI), Todai Institutes
for Advanced Study, The University of Tokyo,
5-1-5 Kashiwa-no-ha, Kashiwa City, Chiba 277-8582, Japan

^dDepartment of Physics, Tokyo Institute of Technology,
2-12-1 Ookayama, Meguro-ku, Tokyo 152-8551, Japan

E-mail: kadota@ibs.re.kr, kawasaki@icrr.u-tokyo.ac.jp,
saikawa@th.phys.titech.ac.jp

Abstract. The next-to-minimal supersymmetric standard model predicts the formation of domain walls due to the spontaneous breaking of the discrete Z_3 -symmetry at the electroweak phase transition, and they collapse before the epoch of big bang nucleosynthesis if there exists a small bias term in the potential which explicitly breaks the discrete symmetry. Signatures of gravitational waves produced from these unstable domain walls are estimated and their parameter dependence is investigated. It is shown that the amplitude of gravitational waves becomes generically large in the decoupling limit, and that their frequency is low enough to be probed in future pulsar timing observations.

Keywords: Cosmic strings, domain walls, monopoles, supersymmetry and cosmology, primordial gravitational waves (theory)

Contents

| | | |
|----------|--|-----------|
| 1 | Introduction | 1 |
| 2 | Higgs potential in the NMSSM | 2 |
| 3 | Domain walls in the NMSSM | 5 |
| 3.1 | Structure of domain walls | 5 |
| 3.2 | Domain wall problem and its solution | 7 |
| 4 | Gravitational waves from domain walls | 9 |
| 5 | Conclusions | 12 |

1 Introduction

Supersymmetry (SUSY) is a well-motivated extension of the standard model (SM) of particle physics involving a solution to the hierarchy problem [see, e.g., [1, 2] for reviews]. The simplest supersymmetric extension of the SM is called the minimal supersymmetric standard model (MSSM), which consists of only SM particles along with a pair of Higgs doublets and their superpartners. Such a model is also motivated by the unification of the gauge forces and the existence of dark matter candidates. These interesting features will be investigated in various upcoming observations including high-energy physics, astrophysics, and cosmology observable.

Aside from the rich phenomenology encountered in the MSSM, it suffers from the so-called μ -problem [3], which is originated from the fact that the superpotential of the MSSM contains a term of the form $\mu H_u H_d$ (called the “ μ -term”) at the tree level. Here H_u and H_d are two Higgs doublet superfields, and μ is some dimensionful parameter. Since the MSSM might be a low energy effective theory derived from a more fundamental theory at higher energies, we naively expect that the magnitude of the μ parameter is of the order of some cutoff scale such as the Planck scale. On the other hand, μ should be of the order of the soft SUSY breaking scale in order to induce the electroweak symmetry breaking appropriately. These considerations seem to revive the hierarchy problem in the MSSM.

The next-to-minimal supersymmetric standard model (NMSSM) [for reviews, see [4, 5]] is one of possible solutions to the μ -problem, which introduces an additional singlet superfield S and replaces the μ -term with the coupling of the form $\lambda S H_u H_d$. Owing to this coupling, an appropriate magnitude of the μ parameter is dynamically generated when the scalar component of the singlet superfield acquires a vacuum expectation value (VEV) at the electroweak phase transition. However, the introduction of the singlet superfield allows the existence of other dimensionful parameters at the tree level. The simplest way to prohibit such additional dimensionful parameters is to impose a discrete Z_3 -symmetry, and such a model is called the Z_3 -invariant NMSSM, or often abridged as the NMSSM.

The discrete Z_3 symmetry of the NMSSM is spontaneously broken when the scalar components of the Higgs fields as well as the singlet scalar acquire VEVs at the electroweak phase transition, which leads to the formation of domain walls in the universe. The existence of such domain walls turns out to be problematic in the standard cosmology [6], and hence it

was argued that the NMSSM is unfavorable from the cosmological point of view [7]. Later, it was pointed out that there are some possibilities to arrange the model to have a small explicit symmetry breaking term, which causes a late time annihilation of the walls [8, 9]. Taking account of these possibilities, we deduce that unstable long-lived domain walls can exist in the early epoch of the universe.

In this paper, we point out that a stochastic background of gravitational waves with observably large amplitude can be produced from domain walls in the NMSSM. The amplitude of gravitational waves is determined once we specify the surface mass density of domain walls and their decay time [10, 11]. Here we estimate the surface mass density by solving nonlinear field equations for the Higgs sector in the NMSSM to find a planar domain wall solution. On the other hand, the peak frequency of gravitational waves solely depends on the decay time scale. We see that the typical frequency of the gravitational waves corresponds to the band which can be probed via pulsar timing observations. Another interesting finding is that the amplitude of gravitational waves becomes generically large in the so-called decoupling limit, where the couplings between the singlet field and Higgs fields become extremely small. Note that, due to the very weak coupling between the singlet-like states and the MSSM sector in the decoupling regime, the signatures such as those from the collider tend to reduce to those in the MSSM, and we emphasize a complementary role of the gravitational waves as a possible probe to distinguish the NMSSM from the MSSM.

Signatures of gravitational waves in the NMSSM were also investigated in Ref. [12] in the context of the first order electroweak phase transition. Differently from that approach, in this paper we focus on the production of gravitational waves from domain walls, which does not depend on the order of the phase transition. The crucial assumption is the occurrence of the spontaneous breaking of a discrete symmetry followed by the late time collapse of domain walls, which is a definite consequence of the NMSSM with the (approximate) Z_3 -symmetry.

The organization of this paper is as follows. In Sec. 2, we describe the scalar potential in the Z_3 -invariant NMSSM, especially focusing on its Higgs sector. In Sec. 3, we introduce a numerical method to analyze the structure of domain walls, and discuss their cosmological evolution. Then, in Sec. 4, we estimate the amplitude and frequency of gravitational waves produced from domain walls and discuss prospects for future observations. Finally, Sec. 5 is devoted to the conclusions.

2 Higgs potential in the NMSSM

Let us consider the supersymmetric standard model with an additional gauge singlet superfield S . As was described in Sec. 1, we impose a discrete Z_3 symmetry, under which every chiral supermultiplet Φ transform as

$$\Phi \rightarrow e^{2\pi i/3} \Phi, \quad (2.1)$$

in order to forbid the presence of dimensionful parameters. The renormalizable superpotential of the NMSSM allowed by the Z_3 symmetry and the gauge invariance can be written as

$$W_{\text{NMSSM}} = \lambda S H_u H_d + \frac{\kappa}{3} S^3 + W_{\text{Yukawa}}, \quad (2.2)$$

where λ and κ are dimensionless couplings, and W_{Yukawa} corresponds to the usual Yukawa couplings of the quark and lepton superfields of the MSSM. In the above equations, contrac-

tion over gauge indices is understood. For instance, we have

$$H_u = \begin{pmatrix} H_u^+ \\ H_u^0 \end{pmatrix}, \quad H_d = \begin{pmatrix} H_d^0 \\ H_d^- \end{pmatrix} \quad (2.3)$$

for $SU(2)_L$ doublet fields, which leads

$$H_u H_d = H_u^+ H_d^- - H_u^0 H_d^0. \quad (2.4)$$

Here and hereafter we use the same symbol for the superfield and its scalar component. From F-term contributions of Eq. (2.2) together with D-term contributions and soft SUSY breaking contributions, we obtain Higgs potential at the tree level:

$$\begin{aligned} V = & |\lambda(H_u^+ H_d^- - H_u^0 H_d^0) + \kappa S^2|^2 + (m_{H_u}^2 + |\lambda|^2 |S|^2)(|H_u^0|^2 + |H_u^+|^2) \\ & + (m_{H_d}^2 + |\lambda|^2 |S|^2)(|H_d^0|^2 + |H_d^-|^2) + \frac{g_1^2 + g_2^2}{8} (|H_u^0|^2 + |H_u^+|^2 - |H_d^0|^2 - |H_d^-|^2)^2 \\ & + \frac{g_2^2}{2} |H_u^+ H_d^{0*} + H_u^0 H_d^{-*}|^2 + m_S^2 |S|^2 + \left[\lambda A_\lambda (H_u^+ H_d^- - H_u^0 H_d^0) S + \frac{1}{3} \kappa A_\kappa S^3 + \text{h.c.} \right], \end{aligned} \quad (2.5)$$

where g_1 and g_2 are the $U(1)_Y$ and $SU(2)_L$ gauge couplings, respectively, and $m_{H_u}^2$, $m_{H_d}^2$, m_S^2 , A_λ , and A_κ are dimensionful soft parameters.

We can rotate away the component H_u^+ by using $SU(2)_L$ transformation, and hereafter we take $H_u^+ = 0$. Furthermore, it is necessary to take $H_d^- = 0$ in order to guarantee that the squared masses of charged components become positive. Therefore, in the following we only consider the potential for the neutral components, and simply denote them as $H_u = H_u^0$ and $H_d = H_d^0$. The scalar potential becomes

$$\begin{aligned} V = & |\kappa S^2 - \lambda H_u H_d|^2 + m_{H_u}^2 |H_u|^2 + m_{H_d}^2 |H_d|^2 + m_S^2 |S|^2 + |\lambda|^2 |S|^2 (|H_u|^2 + |H_d|^2) \\ & + \frac{g^2}{4} (|H_u|^2 - |H_d|^2)^2 + \left[\frac{1}{3} \kappa A_\kappa S^3 - \lambda A_\lambda H_u H_d S + \text{h.c.} \right], \end{aligned} \quad (2.6)$$

where

$$g^2 \equiv \frac{g_1^2 + g_2^2}{2} = \frac{2m_Z^2}{v^2} \simeq 0.275 \quad (2.7)$$

for the Z boson mass $m_Z \simeq 91.2\text{GeV}$ and the Higgs VEV $v \simeq 246\text{GeV}$. Here we assume that there is no explicit CP violation, and take λ , κ , A_λ , and A_κ to be real.

It is possible to take the VEV of $\langle H_u \rangle$ to be real and positive by the use of $U(1)_Y$ transformation. In general, $\langle H_d \rangle$ and $\langle S \rangle$ are complex, but such an extremum becomes always a local maximum if there is no explicit CP violation [13]. Therefore, we can also take $\langle H_d \rangle$ and $\langle S \rangle$ to be real up to the Z_3 transformations.¹ Then, we parameterize three VEVs by using three real quantities:

$$\langle H_u \rangle = \frac{v_u}{\sqrt{2}}, \quad \langle H_d \rangle = \frac{v_d}{\sqrt{2}}, \quad \langle S \rangle = \frac{v_s}{\sqrt{2}}, \quad (2.10)$$

¹If we parameterize general three complex VEVs as

$$\langle H_u \rangle = \frac{1}{\sqrt{2}} v_u e^{i\phi_u}, \quad \langle H_d \rangle = \frac{1}{\sqrt{2}} v_d e^{i\phi_d}, \quad \langle S \rangle = \frac{1}{\sqrt{2}} v_s e^{i\phi_s}, \quad (2.8)$$

with v_u , v_d and v_s being real, relevant CP-violating phases are following two combinations:

$$\theta = \phi_u + \phi_d + \phi_s \quad \text{and} \quad \delta = 3\phi_s. \quad (2.9)$$

with $v_u > 0$. Furthermore, we see that the potential possesses the following symmetries: $\lambda, \kappa, v_s \rightarrow -\lambda, -\kappa, -v_s$ and $\lambda, v_d \rightarrow -\lambda, -v_d$ [14]. Using these symmetries, we fix the signs of λ and v_d to be positive. Other parameters κ, v_s, A_λ , and A_κ can take both signs.

The stationary conditions of the potential $\partial V/\partial H_u = \partial V/\partial H_d = \partial V/\partial S = 0$ lead to

$$\lambda^2(v_s^2 + v_d^2)v_u - \lambda\kappa v_d v_s^2 - \frac{g^2}{2}v_u(v_d^2 - v_u^2) + 2m_{H_u}^2 v_u - \sqrt{2}\lambda A_\lambda v_d v_s = 0, \quad (2.11)$$

$$\lambda^2(v_s^2 + v_u^2)v_d - \lambda\kappa v_u v_s^2 + \frac{g^2}{2}v_d(v_d^2 - v_u^2) + 2m_{H_d}^2 v_d - \sqrt{2}\lambda A_\lambda v_u v_s = 0, \quad (2.12)$$

$$\lambda^2(v_u^2 + v_d^2)v_s + 2\kappa^2 v_s^3 - 2\lambda\kappa v_u v_d v_s + 2m_S^2 v_s - \sqrt{2}\lambda A_\lambda v_u v_d + \sqrt{2}\kappa A_\kappa v_s^2 = 0. \quad (2.13)$$

Once we specify the values of v_u , v_d , and v_s , the soft masses $m_{H_u}^2$, $m_{H_d}^2$, and m_S^2 are determined from Eqs. (2.11)-(2.13):

$$m_{H_u}^2 = -\mu^2 - \frac{\lambda^2}{2}v^2 \cos^2 \beta + \frac{\kappa}{\lambda}\mu^2 \cot \beta + \frac{g^2}{4}v^2 \cos 2\beta + \mu A_\lambda \cot \beta, \quad (2.14)$$

$$m_{H_d}^2 = -\mu^2 - \frac{\lambda^2}{2}v^2 \sin^2 \beta + \frac{\kappa}{\lambda}\mu^2 \tan \beta - \frac{g^2}{4}v^2 \cos 2\beta + \mu A_\lambda \tan \beta, \quad (2.15)$$

$$m_S^2 = -\frac{\lambda^2}{2}v^2 - 2\frac{\kappa^2}{\lambda^2}\mu^2 + \frac{1}{2}\lambda\kappa v^2 \sin 2\beta + \frac{\lambda^2}{4}\frac{A_\lambda v^2}{\mu} \sin 2\beta - \frac{\kappa}{\lambda}\mu A_\kappa, \quad (2.16)$$

where

$$\mu \equiv \frac{\lambda v_s}{\sqrt{2}}, \quad \tan \beta \equiv \frac{v_u}{v_d}, \quad \text{and} \quad v = \sqrt{v_u^2 + v_d^2}. \quad (2.17)$$

Hereafter, we use the following six quantities as free parameters of the model:

$$\lambda, \quad \kappa, \quad A_\lambda, \quad A_\kappa, \quad \tan \beta, \quad \text{and} \quad \mu. \quad (2.18)$$

The definition of the μ -parameter in Eq. (2.17) implies that the value of v_s becomes much larger than the electroweak scale for $\lambda \ll 1$ even though μ takes a value of $\mathcal{O}(100)\text{GeV}$. Such a case is called the decoupling limit, since the coupling between particles associated with the singlet superfield and the MSSM sector becomes negligible for $\lambda \rightarrow 0$. In this limit, dominant terms in the potential (2.6) are given by

$$V \simeq \kappa^2 |S|^4 + m_S^2 |S|^2 + \left[\frac{1}{3}\kappa A_\kappa S^3 + \text{h.c.} \right], \quad (2.19)$$

from which we estimate the value of v_s at the minimum as

$$v_s \simeq -\frac{\sqrt{2}A_\kappa}{4\kappa} \left(1 + \sqrt{1 - \frac{8m_S^2}{A_\kappa^2}} \right). \quad (2.20)$$

Note that the condition $A_\kappa^2 \gtrsim 9m_S^2$ should be satisfied in order that the extremum given by Eq. (2.20) becomes deeper than the other possible minimum with $v_s = 0$ [15]. Assuming that

The no-go theorem of Ref. [13] ensures that these two phases take trivial values at the minimum of the potential. If we fix the $U(1)_Y$ gauge such that $v_u > 0$ and $\phi_u = 0$, this fact implies that there are two more vacua with $(\phi_d, \phi_s) = (2\pi/3, 4\pi/3)$ and $(4\pi/3, 2\pi/3)$ in addition to that given by Eq. (2.10). Note that it is also possible to choose the $U(1)_Y$ gauge such that these three degenerate vacua are represented by $\phi_i = 0, 2\pi/3$, and $4\pi/3$ ($i = u, d, s$), respectively.

the magnitudes of $|A_\kappa|$ and $|m_S|$ are comparable to the soft SUSY breaking mass scale, from Eq. (2.20) we see that a large value of v_s is compatible with $\kappa \ll 1$. Furthermore, it can be shown that κ and λ should be comparable such that the potential does not have unrealistic minima [15, 16]. Therefore, the decoupling limit is given by

$$\lambda \sim \kappa \rightarrow 0 \quad \text{and} \quad v_s \sim -A_\kappa/\kappa \gg \mu, \quad (2.21)$$

with other dimensionful parameters being fixed.

We emphasize that the relation [Eq. (2.21)] does not hold if v_s exceeds some critical value, since there might exist non-renormalizable operators which dominate over $\kappa^2|S|^4$ term in Eq. (2.19) when we make the value of κ sufficiently small. In this regime, the value of v_s is not given by Eq. (2.20), but determined by minimizing the scalar potential including possible non-renormalizable terms. Therefore, we expect that the relation [Eq. (2.21)] remains valid only for some intermediate range of couplings, and that the value of v_s saturates to some finite value for a sufficiently small value of κ .

3 Domain walls in the NMSSM

The Z_3 -symmetry of the potential [Eq. (2.6)] is spontaneously broken when the scalar fields H_u , H_d and S acquire VEVs at the electroweak phase transition. At that time, sheet-like objects called domain walls are created as a consequence of the spontaneous breaking of the discrete symmetry. In this section, we describe the properties of domain walls created in the NMSSM and some theoretical issues related to them. First, we analyze the domain wall solution to estimate the surface mass density in Sec. 3.1. Then, we discuss some cosmological aspects of NMSSM domain walls in Sec. 3.2.

3.1 Structure of domain walls

Since the potential is invariant under the Z_3 transformation [Eq. (2.1)], there exist three degenerate vacua parameterized by $(\langle S \rangle, \langle H_u \rangle, \langle H_d \rangle) = (v_s/\sqrt{2}, v_u/\sqrt{2}, v_d/\sqrt{2})$, $(v_s e^{i2\pi/3}/\sqrt{2}, v_u e^{i2\pi/3}/\sqrt{2}, v_d e^{i2\pi/3}/\sqrt{2})$, and $(v_s e^{i4\pi/3}/\sqrt{2}, v_u e^{i4\pi/3}/\sqrt{2}, v_d e^{i4\pi/3}/\sqrt{2})$. Domain walls are located around boundaries of these three vacua.

In order to find the domain wall solution [i.e., find the spatial configuration of the scalar fields $(S(\mathbf{x}), H_u(\mathbf{x}), H_d(\mathbf{x}))$ around the core of the domain wall], we must solve nonlinear field equations for three complex scalar fields S , H_u and H_d with the potential given by Eq. (2.6). It is straightforward to solve such a system numerically [7, 17]: A planar domain wall solution $(S(z), H_u(z), H_d(z))$ perpendicular to the z -axis can be found from the following equations

$$\frac{d^2S}{dz^2} = \frac{\partial V}{\partial S^*}, \quad \frac{d^2H_u}{dz^2} = \frac{\partial V}{\partial H_u^*}, \quad \text{and} \quad \frac{d^2H_d}{dz^2} = \frac{\partial V}{\partial H_d^*}, \quad (3.1)$$

with boundary conditions

$$(S(z), H_u(z), H_d(z)) \xrightarrow{z \rightarrow -\infty} \left(\frac{v_s}{\sqrt{2}}, \frac{v_u}{\sqrt{2}}, \frac{v_d}{\sqrt{2}} \right),$$

$$(S(z), H_u(z), H_d(z)) \xrightarrow{z \rightarrow +\infty} \left(\frac{v_s e^{i\frac{2\pi}{3}}}{\sqrt{2}}, \frac{v_u e^{i\frac{2\pi}{3}}}{\sqrt{2}}, \frac{v_d e^{i\frac{2\pi}{3}}}{\sqrt{2}} \right). \quad (3.2)$$

Here we use the globally convergent Newton method [18] to solve this boundary value problem. Namely, we first specify the “initial guess” for $(S(z), H_u(z), H_d(z))$ within some finite

interval $-L \leq z \leq L$, and deform it such that Eq. (3.1) is satisfied with an appropriate boundary conditions specified at $z = \pm L$. Then, we iterate this procedure until Eq. (3.1) is satisfied with an accuracy of $\mathcal{O}(10^{-5})$. For an appropriate choice of the initial guess of the functions $(S(z), H_u(z), H_d(z))$, this algorithm converges after a few iteration steps.

Figure 1 shows a typical configuration of the domain wall solution. From Fig. 1 (a) we see that the phases of scalar fields continuously change around the core of the domain walls centered at $z = 0$. We also compute the spatial distribution of the energy density for this solution

$$\begin{aligned} \rho_{\text{wall}}(z) = & \left| \frac{dS}{dz}(z) \right|^2 + \left| \frac{dH_u}{dz}(z) \right|^2 + \left| \frac{dH_d}{dz}(z) \right|^2 \\ & + V(S(z), H_u(z), H_d(z)) - V(v_s/\sqrt{2}, v_u/\sqrt{2}, v_d/\sqrt{2}), \end{aligned} \quad (3.3)$$

where we subtracted a constant term such that $\rho_{\text{wall}} \rightarrow 0$ is satisfied for $z \rightarrow \pm\infty$. As shown in Fig. 1 (b), the energy of the scalar fields is concentrated around the core of the domain wall. Finally, we estimate the surface mass density σ_{wall} of the domain wall by integrating this energy density along the z -axis:

$$\sigma_{\text{wall}} = \int dz \rho_{\text{wall}}(z). \quad (3.4)$$

For a choice of parameters used in Fig. 1, we obtain $\sigma_{\text{wall}} \simeq 1.9 \times 10^9 \text{ GeV}^3$.

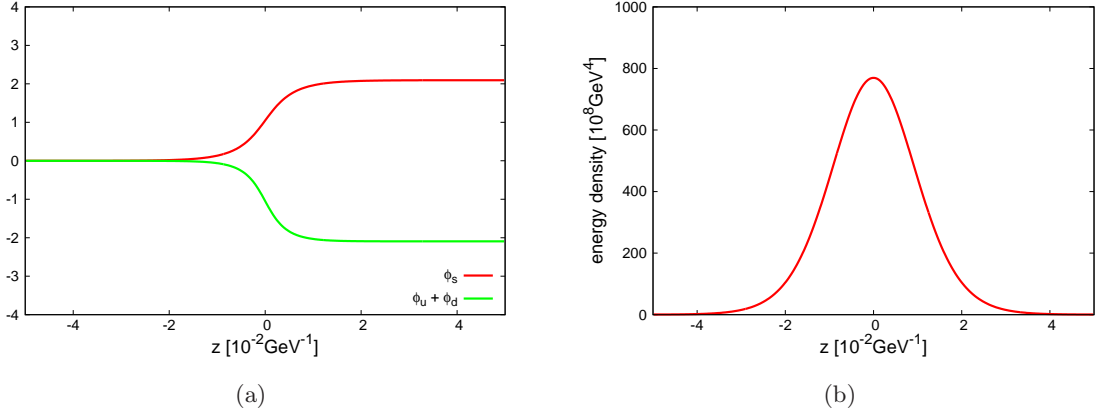


Figure 1. Spatial distribution of (a) phases and (b) energy density of scalar fields $(S(z), H_u(z), H_d(z))$ of the planer domain wall solution for the parameters $\lambda = 0.05$, $\kappa = 0.02$, $A_\lambda = 150 \text{ GeV}$, $A_\kappa = -150 \text{ GeV}$, $\tan \beta = 5$ and $\mu = 200 \text{ GeV}$. In the left panel, ϕ_s , ϕ_u and ϕ_d represent the phases of S , H_u and H_d , respectively. Here we just show the sum of ϕ_u and ϕ_d , since the relative phase between H_u and H_d suffer from an arbitrariness due to the $U(1)_Y$ gauge transformations.

Although the precise value of σ_{wall} can only be calculated by using the numerical procedure, we can roughly estimate the parameter dependence of σ_{wall} in the simple decoupling limit given by Eq. (2.21). Regarding the fact that the phase of the S field continuously changes across the core of the wall and that the potential can be approximated as Eq. (2.19) in the decoupling limit, we expect that the typical length scale of the spatial variation of the field S around the core of the wall is given by $\Delta z \sim |\kappa A_\kappa v_s|^{-1/2}$. Furthermore, the estimation shown in Eq. (2.20) implies that all three terms in the right-hand side of Eq. (2.19) are

comparable, and hence we roughly estimate the height of the potential around the core of the wall as $V \sim |\kappa A_\kappa v_s^3|$. These observations lead to the following scaling behavior of the surface mass density of domain walls:

$$\sigma_{\text{wall}} \sim \kappa v_s^3. \quad (3.5)$$

In fact, we confirmed that this behavior holds very accurately for $\lambda, \kappa < \mathcal{O}(10^{-4})$ in our numerical results. Eq. (3.5) indicates that the surface mass density of domain walls becomes enormously large in the decoupling limit. We will discuss the observational consequence of this property in Sec. 4.

3.2 Domain wall problem and its solution

Let us turn our attention to the cosmological evolution of domain walls. After the formation of domain walls, two kinds of forces act on them. One is the tension force, which smooths out small scale structures to straighten the wall, and the other is the friction force caused by the interactions between particles in the thermal plasma and Higgs fields constituting the wall. The friction force is efficiently induced by particles whose masses are comparable to the electroweak scale, since their interactions with the Higgs fields are relatively strong. However, the number density of these particles drops exponentially as the temperature of the plasma T decreases, and eventually the friction force becomes negligible. The friction effect for the NMSSM domain walls was quantitatively estimated in Ref. [7], and it was shown that this effect becomes irrelevant for $T < \mathcal{O}(0.1\text{--}1)\text{GeV}$.

Once the friction force becomes negligible, the dynamics of domain walls is mostly determined by the tension force, which acts like $p_T \sim \sigma_{\text{wall}}/R_{\text{wall}}$ for a patch of the walls whose typical curvature radius is given by R_{wall} . In this case, it is known that the evolution of domain walls is described by the so-called scaling solution, in which the typical length scales of the system are given by the Hubble radius. In particular, the energy density of domain walls in the scaling regime is given by [10]

$$\rho_{\text{wall}} = \mathcal{A} \frac{\sigma_{\text{wall}}}{t}, \quad (3.6)$$

where \mathcal{A} is a dimensionless coefficient called the area parameter. By comparing a naive estimation $\rho_{\text{wall}} \sim \sigma_{\text{wall}}/R_{\text{wall}}$ with Eq. (3.6), we estimate the typical curvature radius of the walls in the scaling regime as $R_{\text{wall}} \sim t/\mathcal{A}$, and hence the tension force is given by $p_T \sim \mathcal{A}\sigma_{\text{wall}}/t$.

In the literature, the scaling behavior of domain walls [Eq. (3.6)] is confirmed both numerically and analytically [10, 19]. The result of the numerical simulation for the model of a real scalar field with Z_2 symmetry indicates $\mathcal{A} \simeq 0.8 \pm 0.1$ [10], while other simulations for the model with N degenerate vacua show that the value of \mathcal{A} increases proportionally with N [20]. Since we are interested in the model with three degenerate vacua (i.e. Z_3 invariant NMSSM), we simply estimate the value of \mathcal{A} as $\mathcal{A} \simeq 0.8 \times (3/2) = 1.2$.

If the domain walls evolve according to the scaling solution, the decrement of the energy density $\rho_{\text{wall}} \propto 1/t$ is slower than that of dusts $\propto a(t)^{-3}$ and radiations $\propto a(t)^{-4}$, where $a(t)$ is the scale factor of the universe. This fact implies that domain walls are likely to dominate the energy density of the universe at later times. Such an existence of domain walls leads to many problems in the standard cosmological scenario [6].

A simple solution to the domain wall problem is to introduce an additional term ΔV which explicitly breaks the discrete symmetry in the potential [6, 21]. Let us call this additional term a *bias*. We note that the magnitude of the bias term should be much less than

that of the potential around the core of domain walls ($\Delta V \ll V$) such that the discrete Z_3 -symmetry holds approximately. If such a bias term exists in the potential, it breaks the degeneracy between different vacua, and the energy difference between neighboring domains causes the volume pressure $p_V \sim \Delta V$ acting on the walls. Domain walls start to collapse when this pressure p_V exceeds the tension force $p_T \sim \mathcal{A}\sigma_{\text{wall}}/t$, and we can estimate their decay time t_{dec} from the condition $p_V \simeq p_T$:

$$t_{\text{dec}} \simeq \frac{\mathcal{A}\sigma_{\text{wall}}}{\Delta V}. \quad (3.7)$$

If the decay of domain walls occurs before they overclose the universe, we have $\rho_{\text{wall}}(t_{\text{dec}}) < \rho_{\text{crit}}(t_{\text{dec}}) = 3H^2(t_{\text{dec}})/8\pi G$, where $\rho_{\text{crit}}(t_{\text{dec}})$ is the critical density of the universe at the time t_{dec} , $H(t_{\text{dec}})$ is the Hubble parameter at that time, and G is the Newton's constant. From this requirement, we obtain

$$\sigma_{\text{wall}} < 2.93 \times 10^4 \text{TeV}^3 \mathcal{A}^{-1} \left(\frac{0.1 \text{sec}}{t_{\text{dec}}} \right). \quad (3.8)$$

Even if domain walls decay before they overclose the universe, the consideration of big bang nucleosynthesis (BBN) leads to another constraint if they are sufficiently long-lived. For domain walls existing around the epoch of BBN, the ratio between their energy density and the entropy density s is given by

$$\frac{\rho_{\text{wall}}}{s} \simeq 2 \times 10^{-7} \text{GeV} \mathcal{A} \left(\frac{\sigma_{\text{wall}}}{1 \text{TeV}^3} \right) \left(\frac{t}{1 \text{sec}} \right)^{1/2}. \quad (3.9)$$

It is expected that particles radiated from the walls are likely to destroy light elements created during the epoch of BBN. For the abundance of radiated particles, which is comparable with Eq. (3.9), we require $t_{\text{dec}} \lesssim 0.01 \text{sec}$ in order to avoid the constraints on hadronic energy injection in the standard BBN scenario [22]. This condition gives a lower limit on the magnitude of the bias term:

$$\Delta V \gtrsim 6.6 \times 10^{-2} \text{MeV}^4 \mathcal{A} \left(\frac{\sigma_{\text{wall}}}{1 \text{TeV}^3} \right). \quad (3.10)$$

Several remarks on the origin of the bias term [Eq. (3.10)] were made in the literature. A naive expectation is that the discrete symmetry is slightly broken due to gravity, and that a Planck-suppressed higher dimensional operator is responsible for the bias term [23]. However, it turned out that this possibility is unfavorable in the NMSSM [7], since such a Planck-suppressed interaction radiatively induces a tadpole operator [24], which revives the hierarchy problem because of the large VEV of the singlet field. A solution to this problem was proposed in Ref. [8]: It was pointed out that a small tadpole term of the form

$$\Delta V \sim \xi m_{\text{soft}}^3 S + \text{h.c.} \quad (3.11)$$

can be generated by imposing various additional symmetries to constrain the form of non-renormalizable interactions. Here, m_{soft} is the soft SUSY breaking mass, and the dimensionless coefficient ξ corresponds to the loop suppression factor. The term given by Eq. (3.11) is small enough not to destabilize the singlet field, and it acts as a bias term to remove domain walls.²

²We note that there are other various attempts to avoid tadpole and domain wall problem [25–27]. These models also introduce additional symmetries to forbid a large tadpole term. Since the form of the Lagrangian densities of these models becomes different from that of the Z_3 -invariant NMSSM [Eq. (2.2)], which does not lead to the formation of domain walls, we do not consider these possibilities in this paper.

In addition to the solution described above, there is another possibility, where a coupling between the singlet field and additional vector-like matters which are charged under the SM $SU(3)_C$ gauge group or a *hidden* QCD gauge group is introduced [9]. In the presence of such a coupling, the Z_3 -symmetry becomes anomalous for the QCD, and the bias term which destabilizes the domain walls is generated due to the instanton effect [28]. In this case, the magnitude of the bias term is estimated as

$$\Delta V \sim \Lambda^4, \quad (3.12)$$

where Λ corresponds to the QCD scale $\Lambda_{\text{QCD}} \approx \mathcal{O}(100)\text{MeV}$ if vector-like exotics are charged under $SU(3)_C$, or a scale at which the hidden gauge force becomes strong if they are charged under the hidden gauge group.

Once the magnitude of the bias term is specified as Eq. (3.11) or Eq. (3.12), we can estimate the decay time of domain walls according to Eq. (3.7). Since the origin of the bias term is highly model dependent, we take t_{dec} as a free parameter in the rest of this paper.

4 Gravitational waves from domain walls

From the discussion in the previous section, we see that domain walls exist after the electroweak phase transition, and that they collapse before the epoch of BBN $t_{\text{dec}} \lesssim 0.01\text{sec}$ due to the effect of the bias term. In this section, we estimate gravitational wave signatures produced from these unstable domain walls [10, 11, 29].

The cosmological evolution of domain wall networks is accompanied by various violent processes of collisions and annihilations of them. During these processes, a part of the energy stored in them is released as gravitational waves, which leads to a stochastic gravitational wave background observed today. The amplitude of gravitational waves at the cosmic time t for a certain frequency f can be characterized by the following quantity

$$\Omega_{\text{gw}}(t) = \frac{1}{\rho_{\text{crit}}(t)} \frac{d\rho_{\text{gw}}(t)}{d\ln f}, \quad (4.1)$$

where $\rho_{\text{crit}}(t)$ and $\rho_{\text{gw}}(t)$ are the critical density of the universe at the time t and the energy density of gravitational waves at that time, respectively.

The spectrum of gravitational waves from domain walls is estimated in Refs. [10, 11] by the use of 3-dimensional lattice simulation of the scalar field. According to the recent detailed study [10], the spectrum of gravitational waves from domain walls has a peak at the frequency corresponding to the Hubble radius at the time t_{dec} . The peak amplitude of the gravitational waves at that time is given by [10]³

$$\Omega_{\text{gw}}(t_{\text{dec}})_{\text{peak}} = \frac{8\pi\tilde{\epsilon}_{\text{gw}}G^2\mathcal{A}^2\sigma_{\text{wall}}^2}{3H^2(t_{\text{dec}})}, \quad (4.2)$$

where $\tilde{\epsilon}_{\text{gw}}$ is an efficiency parameter of the gravitational radiation. The result of the numerical simulation gives $\tilde{\epsilon}_{\text{gw}} \simeq 0.7 \pm 0.4$ [10]. Assuming that the gravitational radiation is terminated

³In addition to the contribution from the dynamics of domain walls, there exists a secondary background due to the effort of the scalar fields to maintain the scaling defect [30]. The spectrum of such a secondary background turns out to be scale invariant, extending over a wider frequency range. The amplitude of the scale-invariant background $\Omega_{\text{gw}}^{(s)}$ can be estimated from the VEV of the scalar field, and in the NMSSM case we obtain $\Omega_{\text{gw}}^{(s)}(t_{\text{dec}}) \sim (v_s/M_{\text{Pl}})^4$, where $M_P \simeq 1.22 \times 10^{19}\text{GeV}$ is the Planck mass. Since this amplitude is smaller than Eq. (4.2) by a factor of $\sim (H(t_{\text{dec}})/A_\kappa)^2$, hereafter we do not consider this secondary contribution.

in the radiation dominated era, we estimate the amplitude of the gravitational waves at the present time t_0 as

$$\begin{aligned}\Omega_{\text{gw}} h^2(t_0) &\simeq \Omega_R h^2 \left(\frac{g_{S0}}{g_*} \right)^{4/3} \left(\frac{g_0}{g_*} \right)^{1/3} \Omega_{\text{gw}}(t_{\text{dec}}) \\ &\simeq 3.45 \times 10^{-5} \times \left(\frac{10.75}{g_*} \right)^{1/3} \Omega_{\text{gw}}(t_{\text{dec}}),\end{aligned}\quad (4.3)$$

where $\Omega_R h^2 = 4.15 \times 10^{-5}$ is the density parameter of radiations at the present time, h is the present value of the Hubble parameter in the unit of $100 \text{km}\cdot\text{sec}^{-1}\text{Mpc}^{-1}$, $g_{S0} = 3.91$ is the effective degrees of freedom for the entropy density at the present time, and $g_0 = 3.36$ and g_* are the number of radiation degrees of freedom at the present time and t_{dec} , respectively. Substituting Eqs. (3.7) and (4.2) into Eq. (4.3), we obtain

$$\Omega_{\text{gw}} h^2(t_0)_{\text{peak}} \simeq 5.20 \times 10^{-20} \times \tilde{\epsilon}_{\text{gw}} \mathcal{A}^4 \left(\frac{10.75}{g_*} \right)^{1/3} \left(\frac{\sigma_{\text{wall}}}{1 \text{TeV}^3} \right)^4 \left(\frac{1 \text{MeV}^4}{\Delta V} \right)^2. \quad (4.4)$$

The peak frequency is given by the Hubble parameter at the decay time:

$$\begin{aligned}f(t_0)_{\text{peak}} &= \frac{a(t_{\text{dec}})}{a(t_0)} H(t_{\text{dec}}) \\ &\simeq 3.99 \times 10^{-9} \text{Hz} \mathcal{A}^{-1/2} \left(\frac{1 \text{TeV}^3}{\sigma_{\text{wall}}} \right)^{1/2} \left(\frac{\Delta V}{1 \text{MeV}^4} \right)^{1/2}.\end{aligned}\quad (4.5)$$

We see that $\Omega_{\text{gw}} h^2(t_0)_{\text{peak}}$ and $f(t_0)_{\text{peak}}$ are determined by two parameters: σ_{wall} and ΔV [or those appearing in the explicit form of the bias term, i.e., Eq. (3.11) or Eq. (3.12)]. Furthermore, ΔV is related to the decay time of domain walls via Eq. (3.7), and hence Eqs. (4.4) and (4.5) are rephrased as

$$\Omega_{\text{gw}} h^2(t_0)_{\text{peak}} \simeq 1.20 \times 10^{-17} \times \tilde{\epsilon}_{\text{gw}} \mathcal{A}^4 \left(\frac{10.75}{g_*} \right)^{1/3} \left(\frac{\sigma_{\text{wall}}}{1 \text{TeV}^3} \right)^2 \left(\frac{t_{\text{dec}}}{0.01 \text{sec}} \right)^2, \quad (4.6)$$

$$f(t_0)_{\text{peak}} \simeq 1.02 \times 10^{-9} \text{Hz} \left(\frac{0.01 \text{sec}}{t_{\text{dec}}} \right)^{1/2}. \quad (4.7)$$

As was noted in Sec. 3.2, here we use t_{dec} as a free parameter instead of ΔV .

In order to estimate the peak amplitude for a given set of the NMSSM parameters [Eq. (2.18)], we must evaluate the value of the surface mass density of domain walls σ_{wall} appearing in Eq. (4.6). Here, we use the numerical method introduced in Sec. 3.1 to estimate σ_{wall} . Figure 2 shows the estimated peak amplitude in two-dimensional parameter space of (λ, κ) . In this figure, we also plotted some constraints on the tree-level Higgs potential: One is the condition that the mass matrix of seven Higgs scalars (three CP-even, two CP-odd, and a pair of charged states) do not have any negative eigenvalues, and the other is the requirement that the Higgs potential does not lead to unrealistic minima. We used the analytic expression for unrealistic minima obtained in Ref. [16], and checked whether the depth of the desired minimum with $(\langle S \rangle, \langle H_u \rangle, \langle H_d \rangle) = (v_s/\sqrt{2}, v_u/\sqrt{2}, v_d/\sqrt{2})$ is deeper than that of possible unrealistic minima for given values of the parameters (λ, κ) .⁴

⁴An additional constraint might be imposed in order to avoid charged and colored vacua [15]. We do not put this constraint explicitly in Fig. 2, since it also depends on other MSSM parameters such as soft masses for sleptons and squarks.

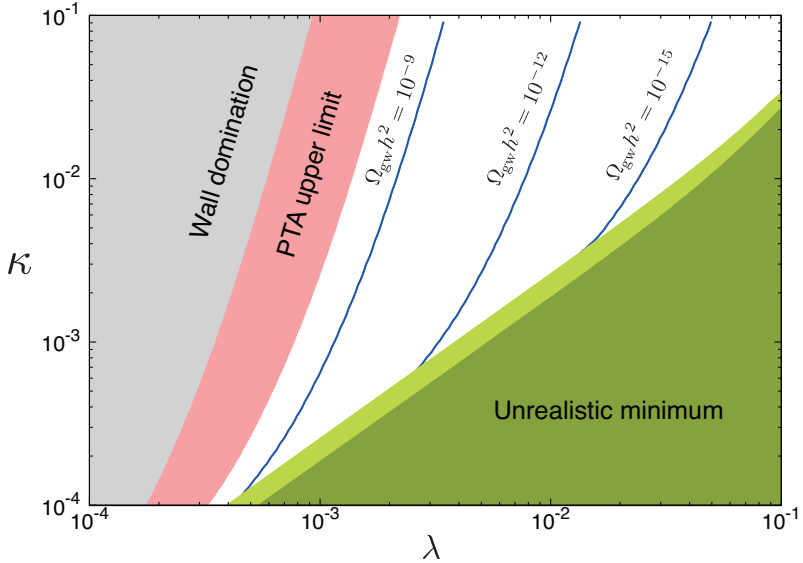


Figure 2. The peak amplitude of gravitational waves estimated from Eq. (4.6) with the assumption of $t_{\text{dec}} = 0.01\text{sec}$ in the (λ, κ) plane. Blue solid lines correspond to contours for $\Omega_{\text{gw}}h^2(t_0)_{\text{peak}} = 10^{-9}$, 10^{-12} , and 10^{-15} . Here we use $g_* = 10.75$, $\mathcal{A} = 1.2$ and $\tilde{\epsilon}_{\text{gw}} = 0.7$ for numerical coefficients appearing in Eq. (4.6). Other theoretical parameters are fixed as $A_\lambda = 150\text{GeV}$, $A_\kappa = -150\text{GeV}$, $\tan \beta = 5$ and $\mu = 200\text{GeV}$. The dark green region corresponds to the parameters at which the mass matrix of Higgs scalars has some negative eigenvalues, and the light green region corresponds to the parameters at which some unrealistic minimum becomes deeper than the desired minimum. The pink region corresponds to the parameter space where the amplitude of gravitational waves exceeds the present limit $\Omega_{\text{gw}}h^2 < 10^{-8}$ from PTA observations. The gray region corresponds to the parameter space where domain walls dominate the energy density of the universe before t_{dec} [i.e. Eq. (3.8)].

The increase in the peak amplitude of gravitational waves for $\lambda \ll 1$ is straightforwardly understood from the relation in the decoupling limit [Eq. (3.5)]. This relation implies that $\Omega_{\text{gw}}h^2(t_0)_{\text{peak}} \propto \kappa^2 v_s^6 t_{\text{dec}}^2 \propto \kappa^2 \lambda^{-6} \mu^6 t_{\text{dec}}^2$ in the limit $\lambda \rightarrow 0$.⁵ We see that the decoupling limit is relevant to the observations, since it generically predicts a large amplitude of gravitational waves. Regarding this fact, in Table 1 we choose some bench mark points in the parameter space, whose predictions can be tested in future experimental research.

There are various ongoing and planned gravitational wave experiments, which aim to detect stochastic gravitational wave backgrounds as well as astrophysical sources. Among them, ground-based interferometers such as (Advanced) LIGO [32], VIRGO [33], KAGRA [34], and ET [35] will probe frequency range around $f \sim 100\text{Hz}$. Space-borne interferometers such as eLISA [36] and DECIGO [37] are also planned to probe lower frequency ranges around 0.1mHz to 10Hz . In addition to these experiments, gravitational wave backgrounds can be probed by using the Pulsar Timing Array (PTA) [38], which is sensitive to the frequency range around $10^{-9}\text{--}10^{-8}\text{Hz}$. Recently, three projects including PPTA, EPTA, and NANOGrav reported upper limit on the stochastic gravitational wave background of $\Omega_{\text{gw}}h^2 < \mathcal{O}(1) \times 10^{-8}$ [39]. As shown in Fig. 2, this present upper limit already excludes some parameter region for

⁵Note that the coupling λ cannot be arbitrary small with keeping the relation in the decoupling limit [Eq. (2.21)], as was discussed at the end of Sec. 2. This fact implies that we cannot extract arbitrarily large amounts of the energy of gravitational waves by simply keeping reducing the coupling λ .

Table 1. Three bench mark points and estimated surface mass density of domain walls, peak amplitude of gravitational waves, and its frequency. Here we used $g_* = 10.75$ for $t_{\text{dec}} = 10^{-2}\text{sec}$ and $g_* = 68.8$ for $t_{\text{dec}} = 10^{-6}\text{sec}$ [31] to estimate $\Omega_{\text{gw}} h^2(t_0)_{\text{peak}}$.

| | I | II | III |
|---|----------------------------------|----------------------------------|----------------------------------|
| λ | 5×10^{-4} | 5×10^{-3} | 5×10^{-6} |
| κ | 2×10^{-4} | 2×10^{-3} | 2×10^{-6} |
| A_λ | 150GeV | 150GeV | 150GeV |
| A_κ | -150GeV | -150GeV | -150GeV |
| $\tan \beta$ | 5 | 5 | 5 |
| μ | 200GeV | 200GeV | 200GeV |
| t_{dec} | 10^{-2}sec | 10^{-2}sec | 10^{-6}sec |
| σ_{wall} | $1.96 \times 10^4 \text{ TeV}^3$ | $1.96 \times 10^2 \text{ TeV}^3$ | $1.96 \times 10^8 \text{ TeV}^3$ |
| $\Omega_{\text{gw}} h^2(t_0)_{\text{peak}}$ | 4.66×10^{-9} | 4.66×10^{-13} | 2.51×10^{-9} |
| $f(t_0)_{\text{peak}}$ | $1.02 \times 10^{-9}\text{Hz}$ | $1.02 \times 10^{-9}\text{Hz}$ | $1.02 \times 10^{-7}\text{Hz}$ |

$t_{\text{dec}} = 0.01\text{sec}$. The future PTA observations such as FAST [40] and SKA [41] will further improve the sensitivities.

Figure 3 shows the schematics of the spectrum of gravitational waves predicted from three points enumerated in Table 1 and sensitivities of planned experiments. The recent result of numerical simulations [10] indicates that the spectrum of gravitational waves from domain walls scales like $\Omega_{\text{gw}} \propto f^3$ for $f < f_{\text{peak}}$ and $\Omega_{\text{gw}} \propto f^{-1}$ for $f > f_{\text{peak}}$, and we also plot this expectation in the figure. We see that the point I leads to the peak at the frequency $f \sim 10^{-9}\text{Hz}$, which can be probed in PTA observations such as SKA. On the other hand, the prediction of the point II indicates that the amplitude gets smaller as the values of λ and κ increase. Interestingly, the spectrum of gravitational waves predicted from the point III might be probed by DECIGO as well as SKA. From these illustrations, we expect that the future PTA observations and space-borne interferometers can probe the signature of gravitational waves from NMSSM domain walls.

5 Conclusions

In this paper, we estimated the gravitational wave signatures from domain walls created at the electroweak phase transition in the NMSSM. The surface mass density of domain walls σ_{wall} is estimated by solving nonlinear equations for Higgs fields numerically. By using the estimated value of σ_{wall} , the amplitude of relic gravitational waves is calculated via Eq. (4.6) and its parameter dependence is explored. We find that a large amplitude of gravitational waves, which scales as $\Omega_{\text{gw}} h_{\text{peak}}^2 \propto \kappa^2 v_s^6 t_{\text{dec}}^2$, is predicted in the decoupling limit. Furthermore, the peak frequency is determined by the decay time of domain walls [Eq. (4.7)], which is related to the magnitude of the bias term ΔV via Eq. (3.7). Such gravitational wave signatures can be probed in the future experiments with improved sensitivities.

We note that the decay time of domain walls t_{dec} is restricted to a certain interval, from the epoch of the electroweak phase transition to that of BBN. The typical frequency of gravitational waves corresponding to such time scales is very low, which is suitable for PTA

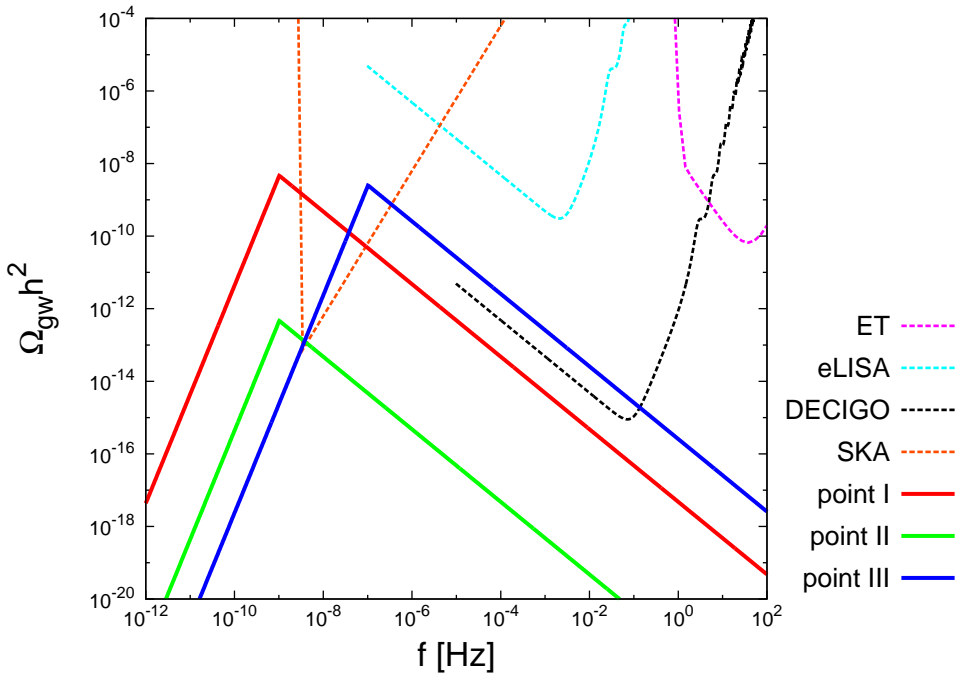


Figure 3. Sensitivity curves of planned detectors (dotted lines) and the spectrum of the gravitational waves produced from domain walls in the NMSSM (solid lines) for various choices of parameters (points I, II, and III) given in Table 1. The sensitivity curve for ET is based on [42], and those for eLISA and (Ultimate) DECIGO are based on [43, 44] [see also Ref. [10]]. The sensitivity of SKA is taken from Ref. [45].

observations. Since the amplitude of gravitational waves becomes large in the decoupling limit, we can use the results of PTA observations as a lower limit on the couplings (λ and κ) appearing in the Higgs sector of the NMSSM. For instance, the present PTA bound $\Omega_{\text{gw}} h^2 \lesssim \mathcal{O}(10^{-8})$ already puts a lower limit $\lambda > 10^{-4}\text{--}10^{-3}$ for $t_{\text{dec}} = 0.01\text{sec}$ (see Fig. 2), while this constraint becomes irrelevant if the decay time of domain walls t_{dec} is earlier than $\mathcal{O}(0.01)\text{sec}$. Future observations will probe a wider range of the parameters in the weak coupling regime, which can be used to complement the results of other experimental studies of the NMSSM.

Acknowledgments

This work was supported by Grant-in-Aid for Scientific research from the Ministry of Education, Science, Sports, and Culture (MEXT), Japan, No. 25400248 (M. K.), World Premier International Research Center Initiative (WPI Initiative), MEXT, Japan. Numerical computation in this work was carried out at the Yukawa Institute Computer Facility. K. K. is supported by Institute for Basic Science (IBS-R018-D1). K. S. is supported by the Japan Society for the Promotion of Science through research fellowships.

References

- [1] H. P. Nilles, Phys.Rept. **110**, 1 (1984).

- [2] S. P. Martin, Adv.Ser.Direct.High Energy Phys. **21**, 1 (2010), [hep-ph/9709356](#).
- [3] J. E. Kim and H. P. Nilles, Phys.Lett. **B138**, 150 (1984).
- [4] M. Maniatis, Int.J.Mod.Phys. **A25**, 3505 (2010), [0906.0777](#).
- [5] U. Ellwanger, C. Hugonie, and A. M. Teixeira, Phys.Rept. **496**, 1 (2010), [0910.1785](#).
- [6] Y. Zeldovich, I. Y. Kobzarev, and L. Okun, Zh.Eksp.Teor.Fiz. **67**, 3 (1974).
- [7] S. Abel, S. Sarkar, and P. White, Nucl.Phys. **B454**, 663 (1995), [hep-ph/9506359](#).
- [8] C. Panagiotakopoulos and K. Tamvakis, Phys.Lett. **B446**, 224 (1999), [hep-ph/9809475](#).
- [9] K. Hamaguchi, K. Nakayama, and N. Yokozaki, Phys.Lett. **B708**, 100 (2012), [1107.4760](#).
- [10] T. Hiramatsu, M. Kawasaki, and K. Saikawa, JCAP **1402**, 031 (2014), [1309.5001](#).
- [11] T. Hiramatsu, M. Kawasaki, and K. Saikawa, JCAP **1005**, 032 (2010), [1002.1555](#); M. Kawasaki and K. Saikawa, JCAP **1109**, 008 (2011), [1102.5628](#).
- [12] R. Apreda, M. Maggiore, A. Nicolis, and A. Riotto, Class.Quant.Grav. **18**, L155 (2001), [hep-ph/0102140](#); R. Apreda, M. Maggiore, A. Nicolis, and A. Riotto, Nucl.Phys. **B631**, 342 (2002), [gr-qc/0107033](#).
- [13] J. Romao, Phys.Lett. **B173**, 309 (1986).
- [14] D. Cerdeno, C. Hugonie, D. Lopez-Fogliani, C. Munoz, and A. Teixeira, JHEP **0412**, 048 (2004), [hep-ph/0408102](#).
- [15] U. Ellwanger, M. Rausch de Traubenberg, and C. A. Savoy, Nucl.Phys. **B492**, 21 (1997), [hep-ph/9611251](#).
- [16] Y. Kanehata, T. Kobayashi, Y. Konishi, O. Seto, and T. Shimomura, Prog.Theor.Phys. **126**, 1051 (2011), [1103.5109](#).
- [17] S. Abel and P. White, Phys.Rev. **D52**, 4371 (1995), [hep-ph/9505241](#).
- [18] W. H. Press, S. A. Teukolsky, W. T. Vetterling, and B. P. Flannery, *Numerical Recipes: The Art of Scientific Computing* (Cambridge University Press, 2007), 3rd ed.
- [19] W. H. Press, B. S. Ryden, and D. N. Spergel, Astrophys.J. **347**, 590 (1989); M. Hindmarsh, Phys.Rev.Lett. **77**, 4495 (1996), [hep-ph/9605332](#); M. Hindmarsh, Phys.Rev. **D68**, 043510 (2003), [hep-ph/0207267](#); T. Garagounis and M. Hindmarsh, Phys.Rev. **D68**, 103506 (2003), [hep-ph/0212359](#); A. Leite and C. Martins, Phys.Rev. **D84**, 103523 (2011), [1110.3486](#); A. Leite, C. Martins, and E. Shellard, Phys.Lett. **B718**, 740 (2013), [1206.6043](#).
- [20] T. Hiramatsu, M. Kawasaki, K. Saikawa, and T. Sekiguchi, JCAP **1301**, 001 (2013), [1207.3166](#); M. Kawasaki, K. Saikawa, and T. Sekiguchi, Phys.Rev. **D91**, 065014 (2015), [1412.0789](#).
- [21] A. Vilenkin, Phys.Rev. **D23**, 852 (1981); P. Sikivie, Phys.Rev.Lett. **48**, 1156 (1982); G. B. Gelmini, M. Gleiser, and E. W. Kolb, Phys.Rev. **D39**, 1558 (1989).
- [22] M. Kawasaki, K. Kohri, and T. Moroi, Phys.Lett. **B625**, 7 (2005), [astro-ph/0402490](#); M. Kawasaki, K. Kohri, and T. Moroi, Phys.Rev. **D71**, 083502 (2005), [astro-ph/0408426](#).
- [23] B. Rai and G. Senjanovic, Phys.Rev. **D49**, 2729 (1994), [hep-ph/9301240](#).
- [24] U. Ellwanger, Phys.Lett. **B133**, 187 (1983); J. Bagger and E. Poppitz, Phys.Rev.Lett. **71**, 2380 (1993), [hep-ph/9307317](#); V. Jain, Phys.Lett. **B351**, 481 (1995), [hep-ph/9407382](#); J. Bagger, E. Poppitz, and L. Randall, Nucl.Phys. **B455**, 59 (1995), [hep-ph/9505244](#).
- [25] S. Abel, Nucl.Phys. **B480**, 55 (1996), [hep-ph/9609323](#).
- [26] C. F. Kolda, S. Pokorski, and N. Polonsky, Phys.Rev.Lett. **80**, 5263 (1998), [hep-ph/9803310](#).
- [27] C. Panagiotakopoulos and K. Tamvakis, Phys.Lett. **B469**, 145 (1999), [hep-ph/9908351](#).

- [28] J. Preskill, S. P. Trivedi, F. Wilczek, and M. B. Wise, Nucl.Phys. **B363**, 207 (1991).
- [29] M. Gleiser and R. Roberts, Phys.Rev.Lett. **81**, 5497 (1998), [astro-ph/9807260](#).
- [30] D. G. Figueroa, M. Hindmarsh, and J. Urrestilla, Phys.Rev.Lett. **110**, 101302 (2013), [1212.5458](#).
- [31] O. Wantz and E. Shellard, Phys.Rev. **D82**, 123508 (2010), [0910.1066](#).
- [32] A. Abramovici, W. E. Althouse, R. W. Drever, Y. Gursel, S. Kawamura, et al., Science **256**, 325 (1992).
- [33] F. Acernese, M. Alshourbagy, P. Amico, F. Antonucci, S. Aoudia, et al., Class.Quant.Grav. **25**, 184001 (2008).
- [34] K. Somiya (KAGRA Collaboration), Class.Quant.Grav. **29**, 124007 (2012), [1111.7185](#).
- [35] B. Sathyaprakash, M. Abernathy, F. Acernese, P. Ajith, B. Allen, et al., Class.Quant.Grav. **29**, 124013 (2012), [1206.0331](#).
- [36] P. Amaro-Seoane, S. Aoudia, S. Babak, P. Binetruy, E. Berti, et al., GW Notes **6**, 4 (2013), [1201.3621](#).
- [37] S. Kawamura, T. Nakamura, M. Ando, N. Seto, K. Tsubono, et al., Class.Quant.Grav. **23**, S125 (2006).
- [38] G. Hobbs, A. Archibald, Z. Arzoumanian, D. Backer, M. Bailes, et al., Class.Quant.Grav. **27**, 084013 (2010), [0911.5206](#).
- [39] F. A. Jenet, G. Hobbs, W. van Straten, R. Manchester, M. Bailes, et al., Astrophys.J. **653**, 1571 (2006), [astro-ph/0609013](#); R. van Haasteren, Y. Levin, G. Janssen, K. Lazaridis, M. Kramer, et al., Mon.Not.Roy.Astron.Soc. **414**, 3117 (2011), [1103.0576](#); P. Demorest, R. Ferdman, M. Gonzalez, D. Nice, S. Ransom, et al., Astrophys.J. **762**, 94 (2013), [1201.6641](#).
- [40] R. Nan, D. Li, C. Jin, Q. Wang, L. Zhu, et al., Int.J.Mod.Phys. **D20**, 989 (2011), [1105.3794](#).
- [41] J. Cordes, M. Kramer, T. Lazio, B. Stappers, D. Backer, et al., New Astron.Rev. **48**, 1413 (2004), [astro-ph/0505555](#).
- [42] URL <https://workarea.et-gw.eu/et/WG4-Astrophysics/base-sensitivity>.
- [43] L. Alabidi, K. Kohri, M. Sasaki, and Y. Sendouda, JCAP **1209**, 017 (2012), [1203.4663](#).
- [44] URL <http://www.srl.caltech.edu/%7Eshane/sensitivity/index.html>.
- [45] A. Sesana and A. Vecchio, Class.Quant.Grav. **27**, 084016 (2010), [1001.3161](#).